Manuscript version: Author's Accepted Manuscript

The version presented in WRAP is the author's accepted manuscript and may differ from the published version or Version of Record.

Persistent WRAP URL:

http://wrap.warwick.ac.uk/110542

How to cite:

Please refer to published version for the most recent bibliographic citation information.
If a published version is known of, the repository item page linked to above, will contain details on accessing it.

Copyright and reuse:

The Warwick Research Archive Portal (WRAP) makes this work by researchers of the University of Warwick available open access under the following conditions.

Copyright © and all moral rights to the version of the paper presented here belong to the individual author(s) and/or other copyright owners. To the extent reasonable and practicable the material made available in WRAP has been checked for eligibility before being made available.

Copies of full items can be used for personal research or study, educational, or not-for-profit purposes without prior permission or charge. Provided that the authors, title and full bibliographic details are credited, a hyperlink and/or URL is given for the original metadata page and the content is not changed in any way.

Publisher's statement:

Please refer to the repository item page, publisher's statement section, for further information.

For more information, please contact the WRAP Team at: wrap@warwick.ac.uk.

warwick.ac.uk/lib-publications

1 **Manganese oxide biomineralization provides protection against**

2 **nitrite toxicity in a cell density dependent manner.**

3

4 Christian Zerfaß[a,b], Joseph A. Christie-Oleza[a,b], and Orkun S. Soyer[a,b,*]

5 [a] School of Life Sciences, BBSRC/EPSRC Warwick Integrative Synthetic Biology Centre (WISB),

6 University of Warwick, Coventry, CV4 7AL, UK. [b] Warwick Integrative Synthetic Biology Centre

7 (WISB), University of Warwick, Coventry, CV4 7AL, UK.

8

9 KEYWORDS: microbial ecology, biomineralization, metal recovery, biotechnology, community

10 function, social behavior, exoenzyme, reactive oxygen species, *Roseoabacter sp.* AzwK-3b.

Corresponding Author

12 * O.Soyer@warwick.ac.uk (O.S.S.)

Author Contributions

14 CZ, JCO and OSS designed the study and the experiments. CZ performed the

15 experiments and analyzed the data. All authors contributed to the writing of the manuscript

16 and have given approval to the final version.

Conflict of Interest

18 The authors declare that there are no conflicts of interest.

19

Abstract

Manganese bio-mineralization is a widespread process among bacteria and fungi. To date there is no conclusive experimental evidence for, how and if this process impacts microbial fitness in the environment. Here we show how a model organism for manganese oxidation is growth-inhibited by nitrite, and that this inhibition is mitigated in presence of manganese. We show that such manganese-mediated mitigation of nitrite-inhibition is dependent on the culture inoculum size and that manganese oxide (MnO_X) forms granular precipitates in the culture, rather than sheaths around individual cells. We provide evidence that MnO_X protection involves both its ability to catalyze nitrite oxidation into (non-toxic) nitrate under physiological conditions, and its potential role in influencing processes involving reactive oxygen species (ROS). Taken together, these results demonstrate improved microbial fitness through MnO_X deposition in an ecological setting, i.e. mitigation of nitrite toxicity, and point to a key role of MnO_X in handling stresses arising from ROS.

Importance

We present here a direct fitness benefit (i.e. growth-advantage) for manganese oxide bio-mineralization activity in *Roseobacter sp.* AzwK-3b, a model organism used to study this process. We find that AzwK-3b in a laboratory culture experiment is growth-inhibited by nitrite in manganese free cultures, while the inhibition is considerably relieved by manganese supplementation and MnO_X formation. We show that biogenic MnO_X interacts directly with nitrite and possibly with reactive oxygen species, and find that its beneficial effects are established through formation of dispersed MnO_X granules in a manner dependent on the population size. These experiments raise the possibility that manganese bio-mineralisation could confer protection against nitrite-toxicity to a population of cells. They open up new avenues of interrogating this process in other species, and provide possible routes to their biotechnological applications, including in metal recovery, biomaterials production, and in synthetic community engineering.

Introduction

A large variety of biominerals based on different cations (e.g. iron, manganese, calcium) and anions (e.g. carbonates, oxides, phosphates) are deposited by different microorganisms (1). One of these is manganese oxide (2–5), which is deposited by the oxidation of soluble Mn^{II}. Microbial Mn^{II} oxidation received attention with the discovery of polymetallic, manganese-rich biogenic deep sea nodules, which have been shown to harbor both manganese-oxidizing, and manganese-reducing organisms (6). While it is suggested that such nodules could potentially be mined for rare earth elements, and the associated metal-active organisms be used in biotechnology of metal recovery (2, 3, 5–8), it remains unclear in many cases why organisms carry out such metal-oxidizing and -reducing activities. In the case of metal-reducing organisms, it has been shown that metabolic energy can be gained under anaerobic conditions from using metal oxides (i.e. manganese, iron, or others) as an alternative terminal electron acceptor (9–11). Some metals can be oxidized by microbes and act as an inorganic energy source for so-called chemolithotrophic growth, as in the case of iron lithotrophy (12). While it has been suggested that manganese oxidation can also be used as a chemolihotrophic source of energy (2), little experimental evidence has been found. In most cases studied, Mn oxidation is not used as a lithotrophic source of energy and, hence, evolutionary advantages of this process are not well understood (2, 7, 8). Two running hypotheses for non-lithotrophic manganese oxidation are that the resulting manganese oxides (MnO_X) can i) increase accessibility of organic nutrients, or ii) protect microbes from potentially toxic compounds and superoxide stress (13, 14). The validity of the former hypothesis remains to be tested conclusively. MnO_X has been shown to react with complex organic (i.e. humic) substances (15), but it is not clear if the resulting organic products form such reactions are utilized by microbes. It is suggested that certain fungi employ ligand-stabilized Mn^{III} to oxidize recalcitrant litter (16), but these studies were not performed with single (defined) carbon/energy sources. The latter hypothesis regarding the protective potential of MnO_X remains unproven to date for metal toxicity (2, 7). It is shown that MnO_X can mediate a protection against superoxides in *Pseudomonas* species (14), but it is not clear how significant this benefit is given that these and other Mn-oxidising species also possess specific superoxide scavenging enzymes such as cataleses and superoxide dismutases (17–19). It has been suggested that MnO_X precipitates can act as strong sorbents of heavy metals,

78 hence mitigating the toxic effects of such metals on microorganisms, but this has yet to be

79 tested in a biological context (2). Taken together, the biological significance of microbial

80 manganese oxidation remains largely a paradox, as no clear benefits have been

81 demonstrated.

82   In recent years, *Roseobacter sp.* AzwK-3b emerged as a model organism to study the

83 generation of MnO_X (20). AzwK-3b is a bacterium that shows significant manganese oxidizing

84 activity in vitro when grown in a complex (rich) K-Medium (20) and defined (acetate-fed) J-

85 medium (21). This activity was shown to be mediated by a secreted exoenzyme - a haem type

86 oxidase - that can catalyze the in vitro generation of superoxides from NADH and oxygen (22)

87 (this and later reactions shown in Figure 1), demonstrating the use of biological reductive

88 energy equivalents. The resulting superoxide can in turn facilitate the Mn^{II} oxidation into

89 Mn^{III}, which undergoes further disproportionation to result in MnO_2 (22–26) – or more

90 specifically mixed valence state MnO_X. While NADH was a suitable electron donor for the in

91 vitro superoxide production by haem peroxidase, the natural reducing agent, and the way it

92 is delivered, is not known. It has been suggested that the haem peroxidase might be loosely

93 membrane-bound (27), which would mean that electrons could be shuttled from cytoplasmic

94 reductive metabolites to the haem peroxidase e.g. via membrane proteins, though would

95 imply that the natural site of superoxide production (and subsequent manganese oxidation)

96 would be in the immediate proximity of the cell. Since haem peroxidases are also found in

97 culture supernatants (22), an extracellular reaction would require that electron donor

98 metabolites are secreted also, which would imply a considerable investment for AzwK-3b.

99 Thus, these mechanistic findings strongly suggest that AzwK-3b is making a significant

100 metabolic investment into production of MnO_X in form of secreted enzymes and possibly also

101 reductive energy donating metabolites. Furthermore, AzwK-3b's cellular and excreted

102 proteome is shown to be different when grown under the presence or absence of Mn, while

103 it is notable that the haem peroxidase described above was not found to be differentially

104 expressed (28). It is currently not clear how and if the metabolically costly process of

105 extracellular Mn oxidation benefits individual cells and how it could have been maintained

106 over evolutionary timescales.

107   In an attempt to better understand any ecologically relevant 'fitness' impacts of

108 manganese oxidation, we have studied the physiology of Roseobacter sp. AzwK-3b in more

109 detail. While we did not find any significant difference in growth rate between manganese-

110 free and -supplemented media, we found that the manganese oxidizing activity of

111 *Roseobacter sp.* AzwK-3b supports growth of the bacterium at nitrite concentrations that fully

112 prevent growth in a manganese-free culture. MnO_X formed as granules dispersed among

113 cells, and its nitrite-inhibition mitigation effects showed a significant population size effect,

114 suggesting a 'community commodity' nature of this compound. Mechanistically, we show

115 that biogenic MnO_X was able to catalyze nitrite oxidation into nitrate under physiological

116 conditions (according to reaction (4) in Figure 1), and that the mitigation of nitrite-inhibition

117 was also affected by NADH. These results suggest that the ability of MnO_X to alleviate nitrite

118 toxicity relates to providing catalytic scavenging of reactive oxygen species (ROS) within the

119 environment, whose effect can be leveraged by nitrite.

120

121 **Results**

122   To study the role of manganese oxidation on microbial fitness we have focused here

123 on *Roseobacter sp.* AzwK-3b, which has recently emerged as a model organism for this

124 process (2, 8). We refer to the oxidation product as MnO_X, since biogenic manganese oxides

125 are usually precipitates with mixed manganese oxidation states, particularly Mn^{II}, Mn^{III} and

126 Mn^{IV} (2, 29). AzwK-3b has been shown to oxidize manganese to MnO_X by means of an

127 exoenzyme and reductive energy (e.g. NADH in vitro), and potentially involving an elaborate

128 redox reaction path (22–26). We first attempted to identify fully-defined growth conditions

129 for this bacterium, which has been to date studied in complex and lean K-medium (20), both

130 of which contained undefined complex ingredients such as peptone or vitamin mixtures and

131 yeast extract (20, 30) or standard vitamin supplements (21). Through systematic analysis of

132 media composition, we have created a minimal defined medium that supports AzwK-3b

133 growth (from now on referred to as modified artificial seawater medium, ASW_m) (Table 1),

134 and that has revealed the requirement for five specific vitamin supplements for growth

135 (Figure S1). Given this defined culture medium, we were then able to interrogate the impact

136 of manganese on the growth of AzwK-3b.

137

Manganese oxidation has negligible impact on growth rate. Despite potentially significant costs associated with exoenzyme secretion and the investment of reductive energy equivalents for superoxide generation, we did not find any substantial difference in growth rates and steady state population sizes with increasing MnII concentration for cultures grown with 25 mM acetate (Figure 2). A slightly slower growth at the highest manganese concentration (500 µM) was observed, but it was difficult to ascertain this effect, as both MnO_X particles and cells co-aggregating with those particles could have interfered with the absorbance measurements. The slightly reduced growth rate at 200 µM $Mn^{II}Cl_2$ is in line with an earlier report on AzwK-3b, where 100 µM Mn^{II} was found to decrease the growth rate in (complex) K-medium (20). Other manganese-oxidizing bacteria, such as *Erythrobacter sp.* SD-21 (31, 32) and a marine *Bacillus* strain (33), were reported to grow better when cultured with Mn^{II}-supplement. In light of these different findings and possible difficulties with growth rate measurements in the presence of manganese precipitation, we cannot be fully conclusive about the growth effects associated with manganese oxidation based on the presented results, however, they are suggestive of a low or no-impact on growth rate.

Manganese oxidation mitigates nitrite growth inhibition. With growth effects being limited, a possible alternative explanation for a positive role of manganese oxidation is a protective effect against inhibitors or stresses (2, 13). Here, we evaluated this hypothesis for nitrite. Nitrite is commonly found in the environment, where it results from the reduction of nitrate, a key terminal electron acceptor utilized by many microbes (34). We found nitrite inhibited the growth of AzwK-3b in manganese-free cultures, where already as little as 0.25 mM nitrite prevented growth of AzwK-3b (Figure 3A). To rule out a salinity effect, different concentrations of sodium chloride were tested (200 mM (default in ASWm) to 428 mM NaCl (default in original ASW medium (35)), and AzwK-3b grew in all tested conditions (Figure S2)

With the addition of 200 µM Mn^{II}, we found that AzwK-3b is able to grow in the presence of up to 1 mM nitrite (Figure 3B). Increasing the nitrite concentration still affected both the growth rate and maximal culture density (based on A_{600}), but this effect was much lower compared to the manganese-free cultures (Figure 3). To overcome any potential confounding effects of MnO_X precipitation on spectroscopic culture density measurements, we additionally quantified acetate consumption by ion chromatography as a proxy for

169   growth. As expected, manganese-free cultures with 0.25 mM (or higher) nitrite showed only

170   insignificant decrease in acetate, while the Mn^{II} supplemented cultures showed acetate

171   consumption in accordance with the A_{600} measurements (see Figure S3). These findings

172   confirm that Mn^{II} supplementation allows AzwK-3b to withstand nitrite inhibition.

173

174   **Nitrite-inhibition relief is a community function that depends on culture size and that is**

175   **mediated by dispersed, granular MnO_X precipitates.** It has been shown that MnO_X

176   precipitation by AzwK-3b is mediated by secreted exoenzymes (22). It is not known, however,

177   whether the process of MnO_X precipitation occurs primarily on individual cell surfaces, or

178   whether it is a population level process with the secreted enzymes conferring to the notion

179   of a "community commodity" (36–39). We hypothesized that these two different scenarios

180   could be distinguished by analyzing population size effects on MnO_X mediated mitigation of

181   nitrite-inhibition. In particular, we designed an experiment in which cultures pre-grown

182   without Mn^{II} are subsequently sub-cultured into media with MnII and nitrite, using different

183   inoculum size. We argue that in the case of MnO_X-based protection being a process confined

184   to individual cells, there should be no effect of inoculation size.

185   We found that MnO_X-based protection against nitrite inhibition was dependent on

186   inoculum size (Figure 4). A pre-culture was grown without nitrite and manganese, and from

187   this, inocula were generated at two different time points within the first third of the

188   exponential phase (labelled IT1 and IT2 in Figure S4). When these inocula were subjected to

189   nitrite in the main-culture, the earlier, low-density inoculum IT1 was inhibited by nitrite

190   regardless of the presence or absence of Mn^{II} (Figure 4 A,B), while manganese-mediated

191   mitigation of nitrite inhibition was clearly evident for the larger, high-density inoculum IT2

192   (Figure 4 C,D). In the IT1 cultures half of the acetate was unused at 0.25 mM nitrite, and

193   gradually more acetate resided with increasing nitrite concentration (Figure S5). In the IT2

194   cultures with Mn^{II} supplementation, however, acetate was completely removed at all nitrite

195   levels below 2.5 mM and only 25 – 50 % of acetate remained at 5 – 10 mM nitrite. In the

196   control samples (no inoculation) there was no change in acetate concentration ruling out any

197   cross-activity with manganese.

198   Rather than a true population size effect, these observed inocula effects could be due

199   to cells from the Mn-free, early-phase pre-cultures not having 'turned on' expression of

200   exoenzymes required for MnO_X precipitation. To rule out this possibility, we performed an

201   additional experiment, where the pre-cultures were already grown with 200 µM Mn^{II}. Using

202   this pre-adapted culture, inocula were again prepared by sampling at different growth time

203   points (IT 1 – 4 in Figure S6, A). Cultures grown from these different inocula displayed much

204   weaker inhibition by increasing nitrite concentrations up to 10 mM (Figure S6, B) and were

205   able to consume acetate (Figure S6, C), yet there were still inoculum size effects on

206   overcoming nitrite inhibition (Figure 5, green). Interestingly, the extent of this effect seems

207   similar to that observed with inocula originating from pre-cultures grown without Mn^{II} but

208   supplied with Mn^{II} after subculturing into nitrite containing media (Figure 5, blue). In

209   particular, at 5 and 10 mM nitrite, maximum growth rate (and final density) data from these

210   two treatments can all be fitted on to a single (sigmoidal) curve that describes the relation

211   between this data and initial inocula density (Figure 5, black line). This shows that the

212   presence of Mn^{II} in the pre-culture does not impact the dynamics of the process, but rather

213   allows the main-culture populations to grow to a higher density under a given nitrite level. In

214   the absence of Mn^{II} in both pre- and main-cultures, a much denser inoculum was required to

215   achieve growth at a given nitrite level and even then both growth rate and final growth

216   density were lower compared to the case in the presence of Mn^{II}. Under this condition, there

217   was still a density dependence of the nitrite effect.

218   These results suggest that MnO_X precipitation is a community level function. To

219   further collaborate on this result, we explored the micro-structure of the AzwK-3b cultures in

220   the presence of Mn^{II}. Analysis of cultures using electron microscopy revealed that MnO_X

221   precipitates as granules dispersed within the culture, and attaching to clusters of cells, rather

222   than forming sheaths around individual cells (as seen in some other cases of metal oxide

223   precipitations (40)) (Figure 6, left). Employing electron dispersive X-ray spectroscopy, we

224   confirmed that these granular structures contained manganese, while no manganese was

225   detected in locations with cells only (i.e. without granular structures, see Figure 6, right).

226

227   **MnO_X mediated nitrite protection involves redox reactions and oxygen radicals.** After

228   establishing the community level functionality of biogenic MnOX as a protective agent against

229   nitrite, we next wanted to evaluate the mechanistic basis of this function in the context of

230   nitrite toxicity. While multiple mechanisms of nitrite-toxicity are reported (41, 42), two key

231 reactive species are usually implicated, i.e. free nitrous acid (43) and peroxynitrite. The former

232 forms through protanation of nitrite, while the latter forms from the reaction of nitrite with

233 hydrogen peroxide (44–46). Thus, two non-exclusive, possible mechanisms of MnO_X relief on

234 nitrite toxicity are: (i) MnO_X catalyzed oxidation of nitrite to nitrate (a reaction that has been

235 shown to be feasible chemically under low pH (47)) and thereby avoiding formation of either

236 free nitrous acid or peroxynitrite; or (ii) MnO_X catalyzed degradation of hydrogen peroxide

237 and thereby avoiding the reaction of this compound with nitrite to form peroxynitrite.

238   To see if AzwK-3b generated MnO_X can catalyze nitrite oxidation under physiological

239 conditions, we collected it from culture supernatants and evaluated its reactivity with nitrite

240 in our ASW_m-medium at pH = 8.0. Over 27 days, we found nitrite oxidation by biogenic MnO_X

241 in a dose dependent manner, while neither synthetic MnO_2 powder nor the MnO_X-free

242 solution showed any significant nitrite oxidation (Figure 7A). The trend of nitrite oxidation

243 matched with nitrate production (Figure 7B), thus confirming the assumed reaction pathway

244 of nitrite-oxidation into nitrate (47). Taking into account the difficulties of accurately

245 determining the amount of precipitated MnO_X that were added into the nitrite assay, we can

246 still estimate that the condition with highest MnO_X levels contained at least 1-2 mM (with

247 respect to Mn). This presents a stoichiometric minimum 2-fold excess over nitrite (at 0.5 mM),

248 hence enough for complete nitrite oxidation. The fact that this reaction didn't proceed further

249 than an oxidation of ~0.18 mM nitrite (i.e. ~35 %) indicates that either the biogenic MnO_X was

250 only partially reactive or that its reactivity reduced over time (as known to be the case for

251 synthetic manganese oxides (2, 13)). Sample pH remained relatively stable with the biogenic

252 MnO_X, while samples without manganese and with synthetic MnO_2 reached a pH of 6.9 and

253 6.8, respectively at the end of the experiment (from an initial pH of 8.2 of the medium). This

254 acidification of the control samples might be due to carbon dioxide dissolution, which might

255 have been buffered in the samples with biogenic MnO_X due to proton consumption during

256 nitrite oxidation, or due to co-precipitated organic solutes (polymers, proteins) from the cell-

257 free supernatant.

258   These findings confirmed that the biogenic MnO_X were capable to oxidize nitrite at

259 physiological conditions, and prompted us to test MnO_X mediated nitrite oxidation directly in

260 AzwK-3b cultures. We found some evidence for decreasing nitrite concentration in different

261 cultures tested, but this was not significant (Figure S7), and some decrease was also seen in

262   the manganese free cultures (indicating possible measurement effects in the solution). If

263   nitrite oxidation was the main mechanism of MnO_X mediated protection in vivo, these

264   cultures would have been expected to oxidize most of the nitrite present in the media. Thus,

265   we conclude that under our experiment conditions nitrite-oxidation was only a potential

266   contributing factor.

267   A plausible alternative mechanism of MnO_X mediated nitrite-inhibition relief could be

268   related to formation of reactive peroxynitrite, which is shown to be highly toxic to bacteria

269   (45, 46, 48, 49), and which can form (particularly) at low pH from the reaction of hydrogen

270   peroxide with nitrite (44). If peroxynitrite is the main species underpinning nitrite toxicity,

271   then MnO_X protection against nitrite could be due to its ability to degrade hydrogen peroxide

272   and thereby reducing the rate of peroxynitrite formation. The reactivity of MnO_X towards

273   hydrogen peroxide has been demonstrated chemically (44, 50–57), but never shown or tested

274   in a biological context. Here, we hypothesized that if these types of redox reactions were

275   involved in MnO_X mediated mitigation of nitrite-inhibition, the process dynamics can be

276   modulated with the introduction of additional hydrogen peroxide or NADH (which can help

277   increase the rate of MnO_X formation (23), but which can also be directly involved in hydrogen

278   peroxide reduction through peroxidase-catalysed reactions (17–19, 58, 59)). To test this

279   hypothesis, we again grew pre-cultures of AzwK-3b without Mn^{II} and sub-cultured these in

280   medium containing Mn^{II} and nitrite, but at the same time also spiking in hydrogen peroxide

281   or NADH. Hydrogen peroxide spiking did not show any effect on nitrite inhibition or its release

282   by Mn^{II} supplementation (Figure S8), possibly due to spiked hydrogen peroxide being cleared

283   primarily through additional peroxidases rather than impacting MnO_X mediated process

284   dynamics. In line with this hypothesis, spiking NADH resulted in full mitigation of nitrite

285   inhibitory effect (even without MnII) (Figure 8). This suggests that nitrite toxicity relates to

286   peroxynitrite formation via hydrogen peroxide, which can be decomposed by MnO_X (as

287   shown before (44, 50–57)) or NADH-utilizing peroxidases (that are shown to be present in

288   *Roseobacter* species including AzwK-3b (22, 27) (see also Table S1)).

289   **Discussion**

290   Manganese bio-mineralization into MnO_X is widespread among bacteria, but there is

291   no clarity about its possible functional roles. Here, we developed a defined growth media for

292   the manganese oxidizing model organism *Roseobacter sp.* AzwK-3b and demonstrated that in

293   a laboratory setting this organism's strong growth-inhibition by nitrite is mitigated through

294   its ability to precipitate biogenic MnO_X. While our experiments were undertaken in an

295   artificial lab environment, these findings provide a direct evidence for the impact of MnO_X on

296   an organism's growth, thus raising the possibility of a positive fitness effect and a possible

297   ecological/evolutionary explanation to the costly process of MnO_X oxidation.

298   Interestingly, we also show that the MnO_X-mediated mitigation of nitrite toxicity is

299   dependent on population size, and that MnO_X forms dispersed granules that are attached to

300   clusters of cells in the population. These observations, combined with the established role of

301   exoenzymes in the formation of MnO_X precipitates, suggests that these provide a community

302   function to AzwK-3b and allows cultures grown to sufficient density in the presence of

303   manganese to become resistant to the inhibitory effects of nitrite. Our attempts to elucidate

304   the mechanistic basis of this functionality showed that biogenic MnO_X can oxidise nitrite to

305   nitrate (under conditions that synthetic MnO_2 cannot). Together with the known ability of

306   MnO_X to degrade hydrogen peroxide (44, 50–57), these findings show that biogenic MnO_X can

307   inhibit the two key routes to the formation of reactive nitrite species.

308   While mitigation of nitrite inhibition might not be the only evolutionary advantage of

309   MnO_X oxidation in AzwK-3b or other manganese oxidizing species, it is definitely an

310   ecologically relevant function. Nitrite is a known inhibitor in the environment (41, 42, 60),

311   including in wastewater treatment applications (43). In soil, reported nitrite concentrations

312   are in the range up to low micromole per kg or litre, respectively (61, 62), though can peak to

313   higher than 0.5 millimole per kg by agricultural nitrogen fertilization (61). In biofilms, where

314   diffusion is inhibited, oxygen is shown to rapidly diminish (63–65), which can favor anaerobic

315   metabolism including nitrate respiration to nitrite (66). Furthermore, biofilms are shown to

316   preferentially select for and accumulate ions such as phosphate and nitrite (67–69). For

317   example, in freshwater lake biofilms, the annual variation range for nitrite was found to be

318   from µM to mM range (i.e. 1,000-fold) in biofilms (68). In the case of AzwK-3b, these physical

319   and ecological processes can be highly relevant, as this species was isolated from an

320   "agriculturally impacted, shallow salt marsh" (20) where nitrite (among other nitrogen

321   species) can occur due to microbial conversion of nitrogen fertilizers (61, 70–72). It is also

322   interesting to note that oceanic manganese-rich modules are found to contain both

323   manganese oxidizing and reducing bacteria (6), with current-day representatives of the latter

324   group, such as *Shewenalla oneidensis* (9), also being nitrate-reducers (73–75). Thus, these

325   nodules can or have harbored also high levels of nitrite, creating environments that select for

326   manganese oxidation.

327   Our study opens up additional investigations into the mechanism of nitrite toxicity and

328   the role of MnO_X oxidation in it. Multiple mechanisms of nitrite-inhibition have been reported

329   (41, 42), and a key role for free nitrous acid (i.e. protonated nitrite) (43) and peroxynitrite,

330   from nitrite and hydrogen peroxide (44–46), is proposed. Both molecules can prevent

331   chemiosmotic coupling, and are primarily formed at low pH (nitrite is often found to inhibit

332   bacterial survival at pH < 7 (45, 46)). Indeed, low pH can arise within the cellular

333   microenvironment: energy metabolism coupled to chemiosmosis generates a proton motive

334   force that can enrich the proton concentration at the charged membrane surface (values

335   down to pH 5.5-6.5 are discussed). This local low pH environment can be further stabilized

336   and inhibited from equilibration with the bulk due to an electrostatic barrier imposed by

337   water layering (76, 77). Additionally, respiratory activity can increase hydrogen peroxide in

338   the same cellular microenvironment (18, 48, 49, 58, 78–85), which can faciliate nitrite

339   conversion to peroxynitrite. Interestingly, these local conditions could be avoided through

340   the presence of MnO_X, which can degrade hydrogen peroxide and catalyse the oxidation of

341   nitrite to nitrate, which is a proton consuming process with increased rate at low pH (47). The

342   latter mechanism is confirmed here under physiological conditions, as we show that biogenic

343   MnO_X can catalyze nitrite oxidation also at pH 8.

344   The MnO_X-mediated hydrogen peroxide degradation as a mechanism to prevent

345   peroxynitrite formation remains to be fully confirmed. Our experiments with spikes of

346   hydrogen peroxide did not alter the gross dynamics of MnO_X mediated nitrite-inhibition relief,

347   but this could be due to the design of these experiments with hydrogen peroxide delivered in

348   single doses rather than being delivered in a controlled manner in the vicinity of the cells. A

349   single dose could have been readily dealt with by additional peroxidases, without altering

350   MnO_X mediated effects. On the other hand, our observation that the nitrite-stress is fully

351   mitigated in NADH- supplemented cultures (even in the absence of MnO_X) lends support to

352   the idea that nitrite stress is mediated primarily through formation of peroxynitrite. In that

353   case, the reductive power of NADH could be employed by peroxidases, as well as MnO_X, to

354 reduce hydrogen peroxide (17, 58, 59) and thereby stopping the formation of peroxynitrite,

355 explaining the observed mitigation effect of NADH.

356   These possible mechanistic scenarios of nitrite toxicity and roles of NADH,

357 peroxidases, and MnO_X in mitigating it, can shed light on why and if manganese oxidation is

358 a functional, actively evolved trait or not. In particular, it is not clear why cells that already

359 have several peroxidases, such as AzwK-3b (22, 27) (see also Table S1), might invest additional

360 energy in the formation of MnO_X precipitates. One possibility is that the the formation of

361 MnO_X is a mere side effect arising from the microbially generated superoxide (which appears

362 widespread among bacteria) (27) reacting with the manganese (Mn^{II}), and the exoenzymes of

363 AzwK-3b simply removing the resulting hydrogen peroxide that would otherwise lead to

364 subsequent reduction of the oxidized manganese (24). An alternative possibility is that

365 manganese oxidation is actively selected for due to the exact reaction mechanisms of ROS

366 scavenging. It has been suggested, for example, that different ROS scavenging enzymes have

367 different substrate affinities and efficiencies (18). In this context MnO_X-mediated scavenging

368 could be preferred under certain ROS concentrations and modes of production. In addition,

369 and unlike peroxidases that require stoichiometric equivalents of reductants as e.g.

370 NADH/NADPH for hydrogen peroxide reduction (18, 19), MnO_X at its different oxidation states

371 (II, III, IV) can, once formed, directly catalyze degradation of hydrogen peroxide without NADH

372 involvement (23, 24, 26, 44, 50–57). The fact that some peroxidases, as well as the AzwK-3b

373 enzyme catalyzing MnO_X formation, are exoenzymes (22, 86) could be also highly relevant.

374 The expression of such exoenzymes is a 'social trait', that can be exploited by cheating cells

375 that do not invest the costs but reap the benefits (36–39). The presented finding that MnO_X

376 forms dispersed granules in the (agitated) liquid culture of AzwK-3b shows that, in this case,

377 the ultimate functional effects arising from exoenzyme activity are localized. This kind of

378 localization is a known strategy to stabilize a social trait in the face of evolution of cheating,

379 as seen in exoenzymes with localized actions involved in sugar degradation (87) and metal

380 scavenging (88). Thus, the reductive energy investment into the formation of MnO_X mediated

381 protection might be a metabolically less costly strategy that is also socially more stable,

382 compared to for example exoenzymes that are freely diffusing.

383   Within a wider context, our findings are relevant to understand the different forms of

384 metal mineralization observed in different microorganisms and under different ecological

385 contexts. Given the abundance of microorganisms being involved in reactions of the nitrogen

386 cycle, there is indeed potential transient accumulation of nitrite in different environments. It

387 is also possible that MnO_X (or other minerals) can provide more broad protection against ROS

388 chemistry. For example, manganese oxidation is also observed in spore-forming bacteria (89,

389 90), fungi and other microorganisms (as reviewed and shown in (2, 40)), where a role for

390 nitrite stress remains to be elucidated. Our findings will facilitate such further studies of bio-

391 mineralizing organisms and their different functional motives and social strategies.

392

Materials and Methods

394 **Bacterial Strain and Culture Conditions.** *Roseobacter sp.* AzwK-3b was obtained from Colleen

395 Hansel (Woods Hole Oceanographic Institution, Falmouth, MA/USA), who isolated the strain

396 (20). Cultures were grown in a defined medium, which was established by modifying the pre-

397 defined artificial seawater (ASW) medium (35). This media is referred to as ASW_m from now

398 on, and its composition is shown in Table 1. ASW_m contained sodium acetate as the sole

399 carbon source (at concentrations specified per experiment), 200mM sodium chloride (instead

400 of 428 mM, as in ASW), ammonium as nitrogen source (instead of nitrate, as in ASW), and five

401 vitamins that were added as supplement. In manganese-supplemented ASWm, manganese

402 chloride ($MnCl_2$) was added to 200 µM. Cultures were grown at 30 °C in appropriate (100 ml)

403 Erlenmeyer flasks (shaking at 150 strokes per minute) or 96 well polystyrene plates (Corning

404 Inc.) closed with lid and parafilm (shaking at 300 strokes per minute). For flask cultures, a

405 MaxQ 4000 shaking incubator (Thermo Fisher Scientific) was used. Plates were incubated in

406 a CLARIOstar plate reader (BMG labtech) and absorbance measurements were done at 600

407 nm (A_{600}) and with path length-correction, so to present absorbance per 1 cm.

408

409 **Electron microscopy (EM) and Energy Dispersive X-ray spectroscopy (EDS) analysis of AzwK-**

410 **3b cultures.** A culture of AzwK-3b (40 ml in 100 ml Erlenmeyer flasks) was inoculated in ASW_m

411 without manganese and nitrite, and containing 50 mM acetate. After 3 days at 150 strokes

412 per minute shaking and 30 °C (by which time the culture reached the stationary phase),

413 dilutions (25x – 200x) were made for a second passage of culture in the same medium,

414 supplemented with 200 µM manganese. After further 2 days of culturing, samples for EM

14

415   were prepared as follows: Cells from 2.5 ml culture were harvested by centrifugation (5 min

416   at 5,000 g), and the supernatant was discarded. From here, several washing and dehydration

417   steps were conducted by re-suspending the pellet in different solutions and subsequently

418   centrifuging for 5 min at 5,000 g (supernatant discarded): (1) first, pellets were twice re-

419   suspended in ASW_m medium basis (no manganese, no acetate, no ammonium, no nitrite, no

420   trace metals); (2) afterwards, samples were re-suspended in 200 µl 70 % ethanol, incubated

421   for 1 min, and pelleted by centrifugation; (3) for a washing-dehydration step, pellets were

422   twice re-suspended in 200 µl 100 % ethanol and harvested by centrifugation; (4) finally,

423   samples were re-suspended in 100 µl of 100 % ethanol. This suspension was then applied to

424   Transmission Electron Microscopy (TEM) grids (Lacey carbon film coated copper grids (Agar

425   Scientific)) by pipetting, in 1 µl portions (allowed to dry in between), until a total of 2 or 5 µl

426   was accumulated (on different grids). After letting dry on the bench overnight, grids were

427   analysed by EM.

428   EM analysis was done on a Gemini SEM 500 (Zeiss) equipped with EDS X-Max detector

429   (Oxford Instruments). Data analysis was done on the associated AZtec software, which

430   contained the spectral information to identify individual elements. Electron micrographs had

431   the best quality in scanning transmission EM mode (STEM) with a high angle annular dark

432   field detector (HAADF). For EDS, the sample needed to be moved, and the HAADF detector

433   had to be withdrawn, so the location of analysis after changing the setup was confirmed by

434   additional scanning EM (SEM) recording. The HAADF recording presented in Figure 6 was

435   recorded at 25 kV and 4.3 mm working distance, with a 50,000 x magnification. The EDS was

436   recorded at 25 kV, and spectra were accumulated for the same time (40 seconds for the two

437   locations compared in Figure 6).

438

439   **Large inocula preparation for nitrite-assays.** AzwK-3b was grown in Erlenmeyer flasks

440   (usually 40 ml culture volume in 100 ml Erlenmeyer flasks) in ASW_m with 25 mM acetate. The

441   culture absorbance A_{600} was recorded regularly on a Spectronic 200 spectrophotometer

442   (Thermo Fisher) with 1 cm path length polystyrene cuvettes, and inocula were sampled at

443   various stages of the growth curve (e.g. see Figures S4, S6, S8). This culture was used to

444   inoculate into 96 well plates, which were supplemented by 1:1 dilution with fresh medium

445   supplemented with manganese and/or nitrite and other additives, as described for the

446   particular results shown (see legends of Figures 4, 6, S6, S8). Where noted (see respective

447   figure captions), the fresh medium used for dilution was also supplemented with NADH or

448   hydrogen peroxide at different concentrations. NADH or hydrogen peroxide were added as

449   last additives (to prevent reaction e.g. between hydrogen peroxide and Mn^{II} before

450   inoculation) and the completed fresh medium was used immediately.

451

452   **Growth curve fitting and analysis.** Growth curves were analyzed using the R-package Grofit

453   (91) applying the Gompertz growth model (91, 92). Plate reader data (measurements every

454   10 minutes) were de-noised by averaging over 6 measurements (i.e. hourly averages). The

455   maximum A_{600} reached was read directly from the data. For curve fitting, all data later than

456   the maximum A_{600}, i.e. decaying growth phase, were removed. Then, the data was read

457   backwards in time to find the first reading that was below 5 % of the maximum A_{600}. This data-

458   trimming was done to facilitate the fitting of the Gompertz growth model without bias from

459   different lag-phases (which were ignored), or different lengths and scales of decaying phases

460   recorded. From the resulting model, the maximum growth rate μ (in A_{600} nm(a.u.) per hour)

461   was recorded.

462

463   **Preparation of cell-free bio-manganese oxide.** The procedure was adapted from previous

464   publications using the cell free supernatant of *Roseobacter sp.* AzwK-3b grown in complex

465   medium (20, 22–24). AzwK-3b was grown in ASW_m supplemented with 50 mM sodium acetate

466   for nine days, using individual 50 or 100 ml cultures in 100 or 200 ml Erlenmeyer flasks,

467   respectively, at 30 °C with shaking (150 strokes per minute). In total, 2 liters of culture was

468   prepared, cells were removed by centrifugation (5 minutes at 10,000 g) and the supernatants

469   were combined. From this (cell-free) supernatant, individual samples of 100 or 200 ml were

470   prepared and supplemented with 200 μM manganese chloride, $MnCl_2$. Manganese oxidation

471   was allowed to proceed for five days at 30 °C with shaking (150 strokes per minute), after

472   which the manganese oxide was harvested by centrifugation (5 minutes at 10,000 g) from

473   each 50/100 ml sample . These were combined and washed by suspending in 25 ml acetate-

474   free ASW_m medium and re-sedimented by centrifugation. The pellet was brown in

475   appearance and had considerable volume, indicating co-precipitation of organic material (e.g.

476   secreted proteins) from the cell-culture supernatant. To estimate the amount of manganese

16

477 precipitated in the assay, the supernatants from centrifugation and the washing steps were

478 combined, and the residual manganese determined by the 3,3',5,5'-tetramethylbenzidine

479 (TMB)-assay (93) for soluble manganese. Note that this was not a precise quantification, but

480 was conclusive enough to allow conservative stoichiometric relations to be inferred. In

481 particular, we inferred that ca. 75 % of the 200 µM manganese chloride had been removed

482 from the solution and this value was used for downstream calculations. The MnO_X precipitate

483 was suspended in an appropriate volume of the acetate-free medium to produce a "10 mM"

484 suspension of manganese oxide, and this value is used in the manuscript as indicator for

485 manganese oxide concentration. The pH was 8.2, which is well in line with the pH 8.0 of the

486 ASW_m medium, showing that the suspended manganese oxide did not alter the pH.

487

488 **Quantification of nitrite, nitrate and acetate.** Quantification was done by Ion

489 Chromatography (IC) on a DIONEX ICS-5000+ (ThermoFisher, UK) equipped with conductivity

490 detector, potassium hydroxide (KOH) eluent generator, appropriate suppressor, and a

491 DIONEX IonPac AS11-HC-4µm (2 x 250 mm ThermoFisher, UK) anion separation column with

492 appropriate guard column. Culture samples were filtered (0.22 µm polyamide spin filter

493 Costar Spin-X, Corning, NY/USA) and 10-fold diluted with MilliQ-water (resistance R > 18.2

494 MΩ), of which 2.5 µl were injected for IC separation. The IC was run as continuous gradient

495 as follows (flow rate 0.38 ml/min, column temperature 30 °C, conductivity detector cell

496 temperature of 35 °C): -7-0 min – 1.5 mM KOH (equilibration), 0-8 min – 1.5 mM KOH, 8-18

497 increase to 15 mM KOH, 18-23 min – increase to 24 mM KOH, 23-24 min – increase to 60 mM

498 KOH, 24-30 min – stay at 60 mM KOH. Reference samples with known concentrations were

499 run for calibration. During the course of the experiments (see below) evaporation of the

500 samples was noted (indicated by the increase in the peak area of chloride, which is expected

501 to be unaltered by any biologic means and therefore should have displayed no concentration

502 change). To correct for this evaporation effect, the concentrations of the analytes of interest

503 were corrected by the same ratio as that obtained from the chloride peak area (from the

504 beginning and end point samples of a particular time-course experiment).

505

Acknowledgments

Conflict of Interest

The authors declare that there are no conflicts of interest.

Supplementary Information

Supplementary information is available at journal's website.

References

519 **References**

520 1.   Lowenstam H. 1981. Minerals formed by organisms. Science 211:1126–1131.

521 2.   Hansel CM. 2017. Manganese in marine microbiology, p. 37–83. *In* Poole, RK (ed.),
522   Advances in Microbial Physiology - Microbiology of Metal Ions. Academic Press, Oxford.

523 3.   Nealson KH. 2006. The manganese-oxidizing bacteria. Prokaryotes 5:222–231.

524 4.   Ghiorse WC. 1984. Biology of iron-and manganese-depositing bacteria. Annu Rev
525   Microbiol 38:515–550.

526 5.   Spiro TG, Bargar JR, Sposito G, Tebo BM. 2010. Bacteriogenic manganese oxides. Acc
527   Chem Res 43:2–9.

528 6.   Blöthe M, Wegorzewski A, Müller C, Simon F, Kuhn T, Schippers A. 2015. Manganese-
529   cycling microbial communities inside deep-sea manganese nodules. Environ Sci
530   Technol 49:7692–7700.

531 7.   Tebo BM, Johnson HA, McCarthy JK, Templeton AS. 2005. Geomicrobiology of
532   manganese(II) oxidation. Trends Microbiol 13:421–428.

533 8.   Geszvain K, Butterfield C, Davis RE, Madison AS, Lee S-W, Parker DL, Soldatova A, Spiro
534   TG, Luther GW, Tebo BM. 2012. The molecular biogeochemistry of manganese(II)
535   oxidation. Biochem Soc Trans 40:1244–1248.

536 9.   Myers CR, Nealson KH. 1988. Bacterial manganese reduction and growth with
537   manganese oxide as the sole electron acceptor. Science 240:1319–21.

538 10. Venkateswaran K, Moser DP, Dollhopf ME, Lies DP, Saffarini DA, MacGregor BJ,
539   Ringelberg DB, White DC, Nishijima M, Sano H, Burghardt J, Stackebrandt E, Nealson
540   KH. 1999. Polyphasic taxonomy of the genus *Shewanella* and description of *Shewanella*
541   *oneidensis sp. nov.* Int J Syst Bacteriol 49:705–24.

542 11. Lovley DR. 1993. Dissimilatory metal reduction. Annu Rev Microbiol 47:263–90.

543 12. Emerson D, Fleming EJ, McBeth JM. 2010. Iron-oxidizing bacteria: an environmental
544   and genomic perspective. Annu Rev Microbiol 64:561–83.

545 13. Remucal CK, Ginder-Vogel M. 2014. A critical review of the reactivity of manganese
546   oxides with organic contaminants. Environ Sci Process Impacts 16:1247–66.

547   14.   Banh A, Chavez V, Doi J, Nguyen A, Hernandez S, Ha V, Jimenez P, Espinoza F, Johnson
548   HA. 2013. Manganese (Mn) Oxidation Increases Intracellular Mn in *Pseudomonas*
549   *putida* GB-1. PLoS One 8:e77835.

550   15.   Sunda WG, Kieber DJ. 1994. Oxidation of humic substances by manganese oxides yields
551   low-molecular-weight organic substrates. Nature 367:62–64.

552   16.   Keiluweit M, Nico P, Harmon ME, Mao J, Pett-Ridge J, Kleber M. 2015. Long-term litter
553   decomposition controlled by manganese redox cycling. Proc Natl Acad Sci 112:E5253–
554   E5260.

555   17.   Farr SB, Kogoma T. 1991. Oxidative stress responses in *Escherichia coli* and *Salmonella*
556   *typhimurium*. Microbiol Rev 55:561–85.

557   18.   Mishra S, Imlay J. 2012. Why do bacteria use so many enzymes to scavenge hydrogen
558   peroxide? Arch Biochem Biophys 525:145–60.

559   19.   Zamocky M, Furtmüller PG, Obinger C. 2008. Evolution of catalases from bacteria to
560   humans. Antioxid Redox Signal 10:1527–1548.

561   20.   Hansel CM, Francis CA. 2006. Coupled photochemical and enzymatic Mn(II) oxidation
562   pathways of a planktonic *Roseobacter*-Like bacterium. Appl Environ Microbiol
563   72:3543–9.

564   21.   Estes ER, Andeer PF, Nordlund D, Wankel SD, Hansel CM. 2017. Biogenic manganese
565   oxides as reservoirs of organic carbon and proteins in terrestrial and marine
566   environments. Geobiology 15:158–172.

567   22.   Andeer PF, Learman DR, McIlvin M, Dunn JA, Hansel CM. 2015. Extracellular haem
568   peroxidases mediate Mn(II) oxidation in a marine *Roseobacter* bacterium via
569   superoxide production. Environ Microbiol 17:3925–3936.

570   23.   Learman DR, Voelker BM, Vazquez-Rodriguez AI, Hansel CM. 2011. Formation of
571   manganese oxides by bacterially generated superoxide. Nat Geosci 4:95–98.

572   24.   Learman DR, Voelker BM, Madden AS, Hansel CM. 2013. Constraints on superoxide
573   mediated formation of manganese oxides. Front Microbiol 4:262.

574   25.   Learman DR, Wankel SD, Webb SM, Martinez N, Madden AS, Hansel CM. 2011. Coupled
575   biotic–abiotic Mn(II) oxidation pathway mediates the formation and structural

576   evolution of biogenic Mn oxides. Geochim Cosmochim Acta 75:6048–6063.

577   26.   Luther GW. 2010. The role of one- and two-electron transfer reactions in forming
578   thermodynamically unstable intermediates as barriers in multi-electron redox
579   reactions. Aquat Geochemistry 16:395–420.

580   27.   Diaz JM, Hansel CM, Voelker BM, Mendes CM, Andeer PF, Zhang T. 2013. Widespread
581   production of extracellular superoxide by heterotrophic bacteria. Science 340:1223–6.

582   28.   Learman DR, Hansel CM. 2014. Comparative proteomics of Mn(II)-oxidizing and non-
583   oxidizing *Roseobacter* clade bacteria reveal an operative manganese transport system
584   but minimal Mn(II)-induced expression of manganese oxidation and antioxidant
585   enzymes. Environ Microbiol Rep 6:501–509.

586   29.   Tebo BM, Bargar JR, Clement BG, Dick GJ, Murray KJ, Parker D, Verity R, Webb SM.
587   2004. Biogenic manganese oxides: properties and mechanisms of formation. Annu Rev
588   Earth Planet Sci 32:287–328.

589   30.   Templeton AS, Staudigel H, Tebo BM. 2005. Diverse Mn(II)-oxidizing bacteria isolated
590   from submarine basalts at Loihi seamount. Geomicrobiol J 22:127–139.

591   31.   Francis CA, Co E-M, Tebo BM. 2001. Enzymatic manganese(II) oxidation by a marine α-
592   proteobacterium. Appl Environ Microbiol 67:4024–4029.

593   32.   Johnson HA, Tebo BM. 2008. In vitro studies indicate a quinone is involved in bacterial
594   Mn(II) oxidation. Arch Microbiol 189:59–69.

595   33.   Wang X, Wiens M, Divekar M, Grebenjuk VA, Schröder HC, Batel R, Müller WEG. 2010.
596   Isolation and characterization of a Mn(II)-oxidizing *Bacillus* strain from the
597   demosponge *Suberites domuncula*. Mar Drugs 9:1–28.

598   34.   Kraft B, Strous M, Tegetmeyer HE. 2011. Microbial nitrate respiration – Genes, enzymes
599   and environmental distribution. J Biotechnol 155:104–117.

600   35.   Wilson WH, Carr NG, Mann NH. 1996. The effect of phosphate status on the kinetics of
601   cyanophage infection in the oceanic cyanobacterium *Synechococcus sp.* WH78031. J
602   Phycol 32:506–516.

603   36.   Cavaliere M, Feng S, Soyer OS, Jiménez JI. 2017. Cooperation in microbial communities
604   and their biotechnological applications. Environ Microbiol 19:2949–2963.

605   37.   Allen B, Gore J, Nowak MA. 2013. Spatial dilemmas of diffusible public goods. Elife
606   2:e01169.

607   38.   West SA, Diggle SP, Buckling A, Gardner A, Griffin AS. 2007. The social lives of microbes.
608   Annu Rev Ecol Evol Syst 38:53–77.

609   39.   Allison SD. 2005. Cheaters, diffusion and nutrients constrain decomposition by
610   microbial enzymes in spatially structured environments. Ecol Lett 8:626–635.

611   40.   Keim CN, Nalini HA, de Lena JC. 2015. Manganese oxide biominerals from freshwater
612   environments in Quadrilatero Ferrifero, Minas Gerais, Brazil. Geomicrobiol J 32:549–
613   559.

614   41.   Cammack R, Joannou C., Cui X-Y, Torres Martinez C, Maraj SR, Hughes MN. 1999. Nitrite
615   and nitrosyl compounds in food preservation. Biochim Biophys Acta - Bioenerg
616   1411:475–488.

617   42.   Müller-Herbst S, Mühlig A, Kabisch J, Rohtraud Pichner, Scherer S. 2015. The food
618   additives nitrite and nitrate and microbiological safety of food products. Am J Microbiol
619   6:1–3.

620   43.   Zhou Y, Oehmen A, Lim M, Vadivelu V, Ng WJ. 2011. The role of nitrite and free nitrous
621   acid (FNA) in wastewater treatment plants. Water Res 45:4672–82.

622   44.   Robinson KM, Beckman JS. 2005. Synthesis of peroxynitrite from nitrite and hydrogen
623   peroxide. Methods Enzymol 207–214.

624   45.   Heaselgrave W, Andrew PW, Kilvington S. 2010. Acidified nitrite enhances hydrogen
625   peroxide disinfection of acanthamoeba, bacteria and fungi. J Antimicrob Chemother
626   65:1207–14.

627   46.   Kono Y, Shibata H, Adachi K, Tanaka K. 1994. Lactate-dependent killing of *Escherichia*
628   *coli* by nitrite plus hydrogen peroxide: a possible role of nitrogen dioxide. Arch Biochem
629   Biophys 311:153–159.

630   47.   Luther, III GW, Popp JI. 2002. Kinetics of the abiotic reduction of polymeric manganese
631   dioxide by nitrite: an anaerobic nitrification reaction. Aquat Geochemistry 8:15–36.

632   48.   Martínez MC, Andriantsitohaina R. 2009. Reactive nitrogen species: molecular
633   mechanisms and potential significance in health and disease. Antioxid Redox Signal

634   11:669–702.

635 49. Tharmalingam S, Alhasawi A, Appanna VP, Lemire J, Appanna VD. 2017. Reactive

636   nitrogen species (RNS)-resistant microbes: adaptation and medical implications. Biol

637   Chem 398:1193–1208.

638 50. Watts RJ, Sarasa J, Loge FJ, Teel AL. 2005. Oxidative and reductive pathways in

639   manganese-catalyzed Fenton's reactions. J Environ Eng 131:158–164.

640 51. Jiang S, Ashton WR, Tseung ACC. 1991. An observation of homogeneous and

641   heterogeneous catalysis processes in the decomposition of H_2O_2 over MnO_2 and

642   $Mn(OH)_2$. J Catal 131:88–93.

643 52. Kanungo SB, Parida KM, Sant BR. 1981. Studies on MnO_2—III. The kinetics and the

644   mechanism for the catalytic decomposition of H_2O_2 over different crystalline

645   modifications of MnO_2. Electrochim Acta 26:1157–1167.

646 53. Rophael MW, Petro NS, Khalil LB. 1988. II — kinetics of the catalytic decomposition of

647   hydrogen peroxide solution by manganese dioxide samples. J Power Sources 22:149–

648   161.

649 54. Do S-H, Batchelor B, Lee H-K, Kong S-H. 2009. Hydrogen peroxide decomposition on

650   manganese oxide (pyrolusite): Kinetics, intermediates, and mechanism. Chemosphere

651   75:8–12.

652 55. Li W, Liu Z, Liu C, Guan Y, Ren J, Qu X. 2017. Manganese dioxide nanozymes as

653   responsive cytoprotective shells for individual living cell encapsulation. Angew Chem

654   Int Ed Engl 56:13661–13665.

655 56. Broughton DB, Wentworth RL. 1947. Mechanism of decomposition of hydrogen

656   peroxide solutions with manganese dioxide. I. J Am Chem Soc 69:741–744.

657 57. Broughton DB, Wentworth RL, Laing ME. 1947. Mechanism of decomposition of

658   hydrogen peroxide solutions with manganese dioxide. II. J Am Chem Soc 69:744–747.

659 58. Seaver LC, Imlay JA. 2001. Alkyl hydroperoxide reductase is the primary scavenger of

660   endogenous hydrogen peroxide in *Escherichia coli*. J Bacteriol 183:7173–7181.

661 59. Nathan C, Bryk R, Griffin P. 2000. Peroxynitrite reductase activity of bacterial

662   peroxiredoxins. Nature 407:211–215.

663   60.   Camargo JA, Alonso A. 2006. Ecological and toxicological effects of inorganic nitrogen
664   pollution in aquatic ecosystems: A global assessment. Environ Int 32:831–49.

665   61.   Cleemput O, Samater AH. 1995. Nitrite in soils: accumulation and role in the formation
666   of gaseous N compounds. Fertil Res 45:81–89.

667   62.   Homyak PM, Vasquez KT, Sickman JO, Parker DR, Schimel JP. 2015. Improving Nitrite
668   Analysis in Soils: Drawbacks of the Conventional 2 M KCl Extraction. Soil Sci Soc Am J
669   79:1237.

670   63.   Peters AC, Wimpenny JWT, Coombs JP. 1987. Oxygen profiles in, and in the agar
671   beneath, colonies of *Bacillus cereus*, *Staphylococcus albus* and *Escherichia coli*.
672   Microbiology 133:1257–1263.

673   64.   Jiang X, Zerfaß C, Feng S, Eichmann R, Asally M, Schäfer P, Soyer OS. 2018. Impact of
674   spatial organization on a novel auxotrophic interaction among soil microbes. ISME J
675   12:1443–1456.

676   65.   Dietrich LEP, Okegbe C, Price-Whelan A, Sakhtah H, Hunter RC, Newman DK. 2013.
677   Bacterial Community Morphogenesis Is Intimately Linked to the Intracellular Redox
678   State. J Bacteriol 195:1371–1380.

679   66.   Stewart PS. 2003. Diffusion in Biofilms. J Bacteriol 185:1485–1491.

680   67.   Tsuchiya Y, Eda S, Kiriyama C, Asada T, Morisaki H. 2016. Analysis of Dissolved Organic
681   Nutrients in the Interstitial Water of Natural Biofilms. Microb Ecol 72:85–95.

682   68.   Tsuchiya Y, Ikenaga M, Kurniawan A, Hiraki A, Arakawa T, Kusakabe R, Morisaki H. 2009.
683   Nutrient-rich microhabitats within biofilms are synchronized with the external
684   environment. Microbes Environ 24:43–51.

685   69.   Kurniawan A, Yamamoto T, Tsuchiya Y, Morisaki H. 2012. Analysis of the Ion
686   Adsorption-Desorption Characteristics of Biofilm Matrices. Microbes Environ 27:399–
687   406.

688   70.   Riley WJ, Ortiz-Monasterio I, Matson PA. 2001. Nitrogen leaching and soil nitrate,
689   nitrite, and ammonium levels under irrigated wheat in Northern Mexico. Nutr Cycl
690   Agroecosystems 61:223–236.

691   71.   Lawniczak AE, Zbierska J, Nowak B, Achtenberg K, Grześkowiak A, Kanas K. 2016.

692   Impact of agriculture and land use on nitrate contamination in groundwater and
693   running waters in central-west Poland. Environ Monit Assess 188:172.

694 72. Beeckman F, Motte H, Beeckman T. 2018. Nitrification in agricultural soils: impact,
695   actors and mitigation. Curr Opin Biotechnol 50:166–173.

696 73. Cruz-García C, Murray AE, Klappenbach JA, Stewart V, Tiedje JM. 2007. Respiratory
697   nitrate ammonification by *Shewanella oneidensis* MR-1. J Bacteriol 189:656–662.

698 74. Chen Y, Wang F. 2015. Insights on nitrate respiration by *Shewanella*. Front Mar Sci 1:80.

699 75. Zhang H, Fu H, Wang J, Sun L, Jiang Y, Zhang L, Gao H. 2013. Impacts of Nitrate and
700   Nitrite on Physiology of *Shewanella oneidensis*. PLoS One 8:e62629.

701 76. Mulkidjanian AY, Heberle J, Cherepanov DA. 2006. Protons @ interfaces: Implications
702   for biological energy conversion. Biochim Biophys Acta - Bioenerg 1757:913–930.

703 77. Busch KB, Deckers-Hebestreit G, Hanke GT, Mulkidjanian AY. 2013. Dynamics of
704   bioenergetic microcompartments. Biol Chem 394.

705 78. van der Heijden J, Vogt SL, Reynolds LA, Peña-Díaz J, Tupin A, Aussel L, Finlay BB. 2016.
706   Exploring the redox balance inside gram-negative bacteria with redox-sensitive GFP.
707   Free Radic Biol Med 91:34–44.

708 79. Seaver LC, Imlay JA. 2001. Hydrogen peroxide fluxes and compartmentalization inside
709   growing *Escherichia coli*. J Bacteriol 183:7182–7189.

710 80. González-Flecha B, Demple B. 1995. Metabolic sources of hydrogen peroxide in
711   aerobically growing *Escherichia coli*. J Biol Chem 270:13681–13687.

712 81. Gutteridge JM. 1994. Biological origin of free radicals, and mechanisms of antioxidant
713   protection. Chem Biol Interact 91:133–40.

714 82. Quijano C, Trujillo M, Castro L, Trostchansky A. 2016. Interplay between oxidant
715   species and energy metabolism. Redox Biol 8:28–42.

716 83. Davies KJ. 1995. Oxidative stress: the paradox of aerobic life. Biochem Soc Symp 61:1–
717   31.

718 84. Korshunov S, Imlay JA. 2010. Two sources of endogenous hydrogen peroxide in
719   *Escherichia coli*. Mol Microbiol 75:1389–1401.

720 85. van der Heijden J, Vogt SL, Reynolds LA, Peña-Díaz J, Tupin A, Aussel L, Finlay BB. 2016.
721 Analysis of bacterial survival after exposure to reactive oxygen species or antibiotics.
722 Data Br 7:894–899.

723 86. Christie-Oleza JA, Scanlan DJ, Armengaud J. 2015. "You produce while I clean up", a
724 strategy revealed by exoproteomics during *Synechococcus - Roseobacter* interactions.
725 Proteomics 15:3454–3462.

726 87. Gore J, Youk H, van Oudenaarden A. 2009. Snowdrift game dynamics and facultative
727 cheating in yeast. Nature 459:253–6.

728 88. Kümmerli R, Jiricny N, Clarke LS, West SA, Griffin AS. 2009. Phenotypic plasticity of a
729 cooperative behaviour in bacteria. J Evol Biol 22:589–98.

730 89. Francis CA, Tebo BM. 2002. Enzymatic manganese(II) oxidation by metabolically
731 dormant spores of diverse *Bacillus* species. Appl Environ Microbiol 68:874–880.

732 90. Bargar J., Tebo B., Villinski J. 2000. In situ characterization of Mn(II) oxidation by spores
733 of the marine *Bacillus sp.* strain SG-1. Geochim Cosmochim Acta 64:2775–2778.

734 91. Kahm M, Hasenbrink G, Lichtenberg-Fraté H, Ludwig J, Kschischo M. 2010. Grofit: fitting
735 biological growth curves with R. J Stat Softw 33:1–21.

736 92. Zwietering MH, Jongenburger I, Rombouts FM, van 't Riet K. 1990. Modeling of the
737 bacterial growth curve. Appl Environ Microbiol 56:1875–81.

738 93. Bosch Serrat F. 1998. 3,3',5,5'-Tetramethylbenzidine for the colorimetric
739 determination of manganese in water. Mikrochim Acta 129:77–80.

740 94. Tang YJ, Laidlaw D, Gani K, Keasling JD. 2006. Evaluation of the effects of various culture
741 conditions on Cr(VI) reduction by *Shewanella oneidensis* MR-1 in a novel high-
742 throughput mini-bioreactor. Biotechnol Bioeng 95:176–184.

743 95. Balch WE, Fox GE, Magrum LJ, Woese CR, Wolfe RS. 1979. Methanogens: reevaluation
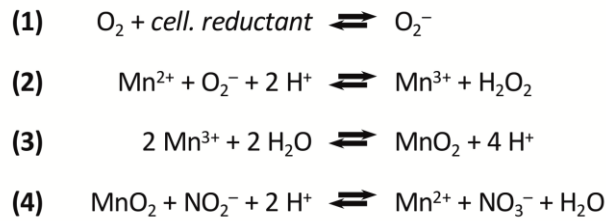744 of a unique biological group. Microbiol Rev 43:260–96.

745

746

Tables

Table 1. Detailed composition of the defined AzwK-3b growth medium, ASW_m. The medium

was developed starting out from artificial seawater (ASW) (35) with extra trace metals taken

from (9, 94) and a 5-vitamin solution identified starting out from Wolfe's vitamin mixture (95).

Compound	Concentration
Base salts (1 x AzwK-3b medium)	
Sodium chloride (NaCl)	200 mM
Ammonium chloride (NH_4Cl)	8.82 mM
Potassium chloride (KCl)	6.71 mM
di-potassium hydrogenphosphate (KH_2PO_4)	131 μM
Magnesium sulphate ($MgSO_4$)	14.2 mM
Magnesium chloride ($MgCl_2$)	9.84 mM
Calcium chloride ($CaCl_2$)	3 mM
Tris(hydroxymethyl)aminomethane (TRIS)	1.1 mM
pH of the medium	**8.0**
Trace metal solution (1,000 x)	
Copper chloride ($CuCl_2$)	32 μM
Zink sulphate ($ZnSO_4$)	765 μM
Cobalt chloride ($CoCl_2$)	169 μM
Sodium molybdate (Na_2MoO_4)	1.65 mM
Boric acid (H_3BO_3)	46.3 mM
Nickel chloride ($NiCl_2$)	4.2 mM
Sodium tungstate (Na_2WoO_4)	243 μM
Sodium selenite (Na_2SeO_3)	228 μM
Additional (1,000 x) supplement solutions	
Iron chloride ($FeCl_3$; prepared in 10 mM HCl, balanced with extra 10 mM NaOH solution)	10.4 mM
Ethylenediaminetetraacetate (EDTA, pH 8.0; sodium salt)	1.34 mM
Manganese chloride ($MnCl_2$, only added where desired)	200 mM
Vitamin supplement (1,000 x)	
Biotin	82 μM
Pyridoxine hydrochloride	484 μM
Thiamine hydrochloride	148 μM
Riboflavin	133 μM
Nicotinic acid	406 μM

752

Figures

$$\textbf{(1)} \quad O_2 + \textit{cell. reductant} \rightleftharpoons O_2^-$$

$$\textbf{(2)} \quad Mn^{2+} + O_2^- + 2\,H^+ \rightleftharpoons Mn^{3+} + H_2O_2$$

$$\textbf{(3)} \quad 2\,Mn^{3+} + 2\,H_2O \rightleftharpoons MnO_2 + 4\,H^+$$

$$\textbf{(4)} \quad MnO_2 + NO_2^- + 2\,H^+ \rightleftharpoons Mn^{2+} + NO_3^- + H_2O$$

Figure 1. Biological oxidation of manganese via superoxide, and nitrite oxidation by the

product manganese oxide. These reactions are taken from references (24) (manganese

oxidation) and (47) (nitrite oxidation). Note that only representative reactions are presented.

For instance, the text refers to a mixed oxide (MnO_X), while this reaction scheme simplyfies

to MnO_2. The cellular reductant (*cell. reductant*) which serves as electron donor for

superoxide production is not unambiguously identified.
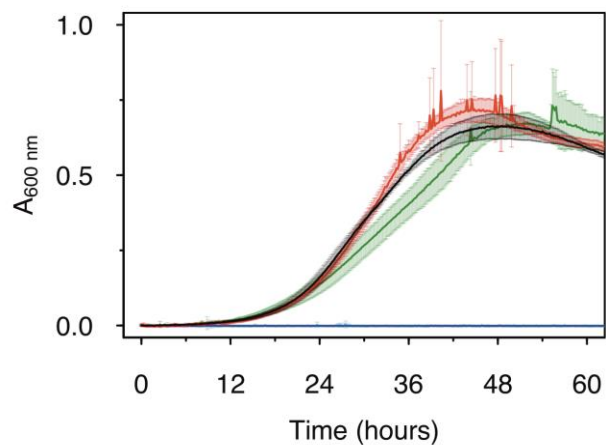
Figure 2. Effect of Mn^{II} on the growth of *Roseobacter sp.* AzwK-3b in the defined growth

medium (see Table 1). The concentrations of manganese were 0 µM (black), 200 µM (red)

and 500 µM (dark green), with no growth (zero line) in the respective non-inoculated controls

(blue, magenta, light blue). Cultures were grown in a 96 well plate (200 µl culture) with

shaking and absorbance measurement every 10 minutes (see Methods).

770
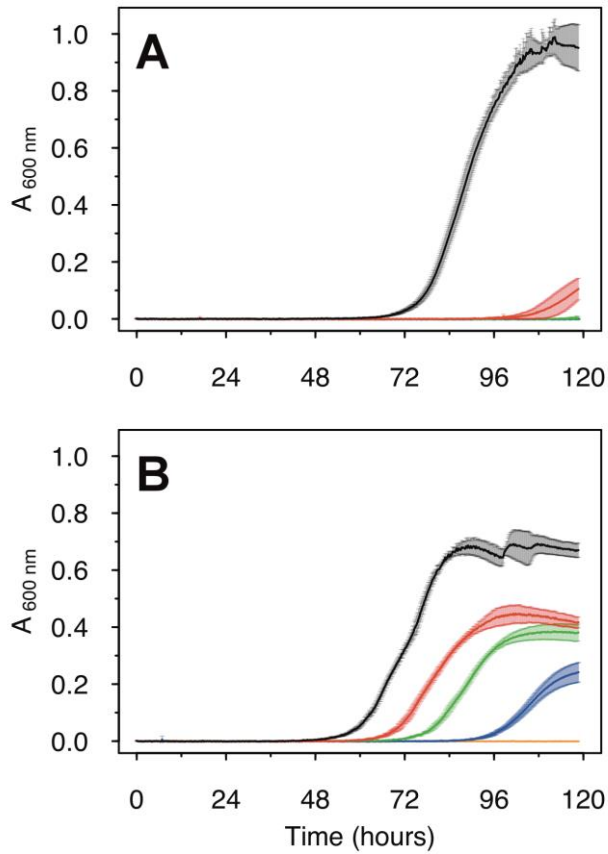
Figure 3. Growth of *Roseobacter sp.* AzwK-3b in the defined growth medium supplemented with sodium nitrite. Media were prepared without (Figure A) or with (Figure B) 200 µM manganese chloride, $Mn^{II}Cl_2$. Nitrite-concentrations were 0 mM (black), 0.25 mM (red), 0.5 mM (green), 1 mM (dark blue) and 2.5 mM (light blue). All conditions were tested in triplicates, and the growth curves represent averages and their standard deviations (see Methods).

777
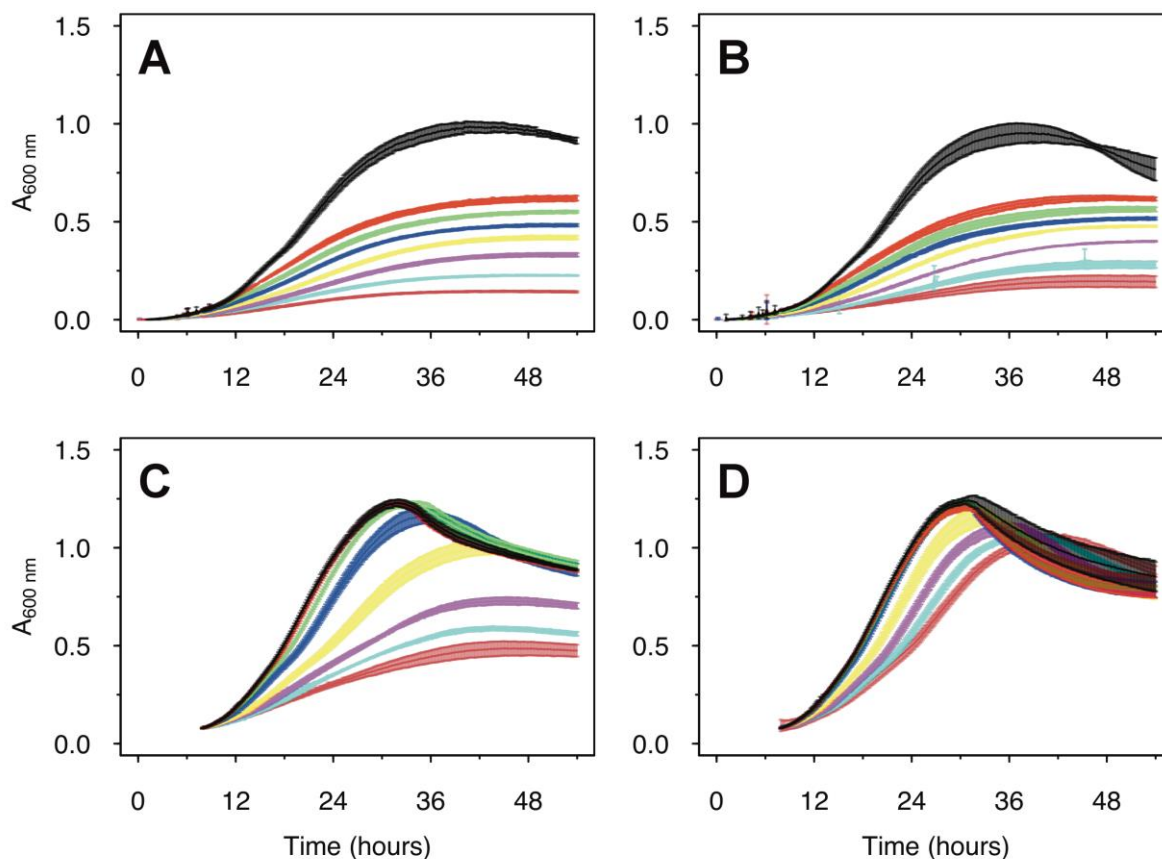
Figure 4. Larger AzwK-3b inocula are less inhibited by nitrite. A pre-culture without manganese or nitrite was grown and sampled in the exponential growth phase (Figure S4) to prepare inocula from a very early time point in the exponential phase (IT 1, Figures A and B), and from a later time point (IT 2, Figures C and D; both sampled in first third of exponential phase). These inocula were 1:1 diluted with fresh medium, and tested for growth at different nitrite concentrations (see below for colour code) without (A, C) or with (B, D) 200 µM Mn^{II}Cl$_2$ supplement. The nitrite concentrations were: Black – control no nitrite. Red – 0.25 mM nitrite. Green – 0.5 mM nitrite. Blue – 1 mM nitrite. Yellow – 2 mM nitrite. Magenta – 5 mM nitrite. Light blue – 7.5 mM nitrite. Dark red – 10 mM nitrite. Growth curves show the averages and standard deviations over a triplicate analysis (see Methods).
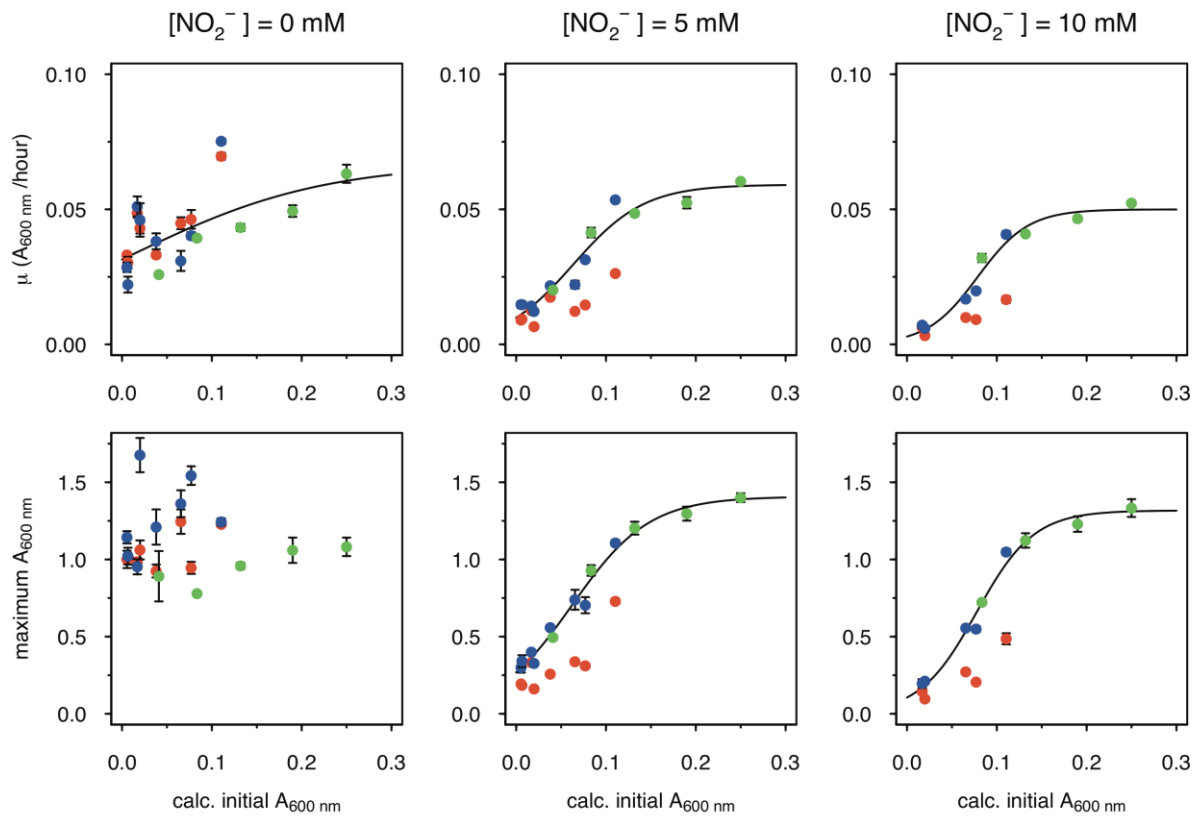
Figure 5. Inoculum-size effect on MnO_X mediated mitigation of nitrite-inhibition. Data from different AzwK-3b growth experiments of similar type ("Large inocula", see *Methods*) were analyzed for the maximum A_{600} (bottom row) and growth rate (top row) by fitting the growth curves. Each condition was done in three technical replicates (note that error bars are not visible in some cases due to only small differences). Nitrite-concentrations of the main-cultures are indicated as headings of the figure-columns. The x-axes show the calculated A_{600} of the initial cultures after diluting them 1:1 from the pre-cultures, while the y-axes show the maximum A_{600} and maximum growth rate as calculated with the Gompertz model (91, 92)) (see *Methods*). The colours represent different conditions: **Red:** Neither pre-, nor main-culture contained manganese; **Blue:** Pre-culture without, main-culture with manganese; **Green:** both pre- and main-culture with manganese. The black curve is a sigmoidal fit (logistic model) from the Grofit R-package (91), for the results of the combined blue and green dataset where the nitrite-exposed main-cultures all contained manganese.
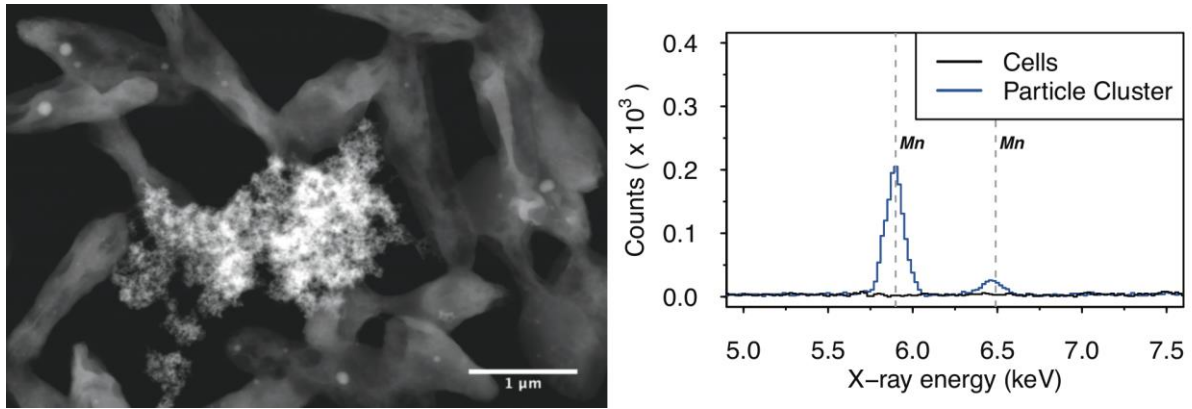
Figure 6. Scanning transmission electron micrograph (left figure, high angle annular dark field) of (granular) manganese-containing precipitate (center) surrounded by AzwK-3b cells, and associated energy dispersive X-ray spectroscopic analysis (right figure) in this location. Only the energy range containing the manganese-specific X-ray energies at 5.90 keV (K_α^I) and 6.49 keV (K_β^I) is shown, and the manganese transitions are indicated by vertical gray dashed lines.

812
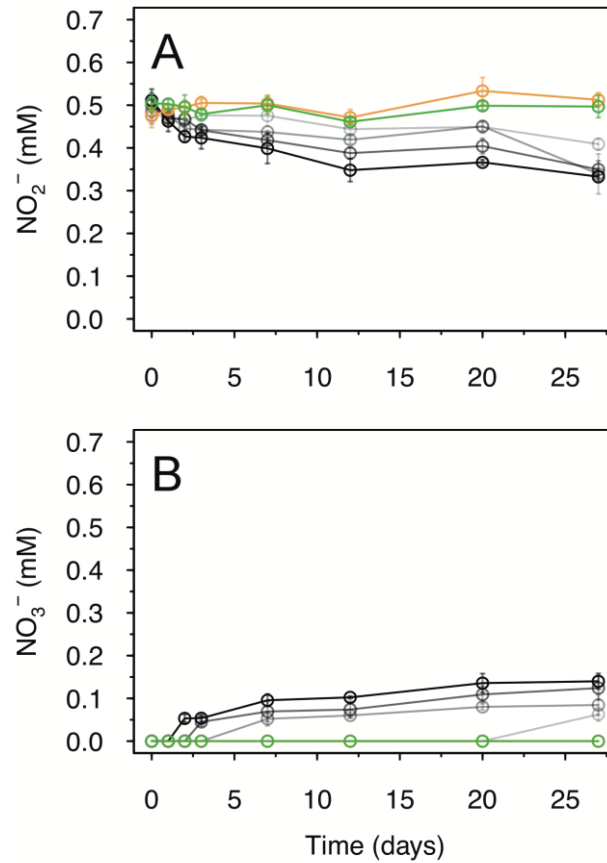
Figure 7. Oxidation of nitrite by biogenic manganese oxide (MnO$_X$) produced in cell-freeculture supernatant of AzwK-3b. The figures show the concentration of nitrite (A) and nitrate (B), determined by ion chromatography, over time (note that concentrations were corrected for the IC-peak from chloride, to account for evaporation during the experiment). As controls, samples without MnO$_X$ (green), or with MnO$_2$ powder (orange) were included in the experiment (see Methods). The samples with AzwK-3b cell-free manganese oxide contained (from grey to black) 0.2, 0.5, 1 and 2 mM manganese oxide equivalent (see Methods).

821

822
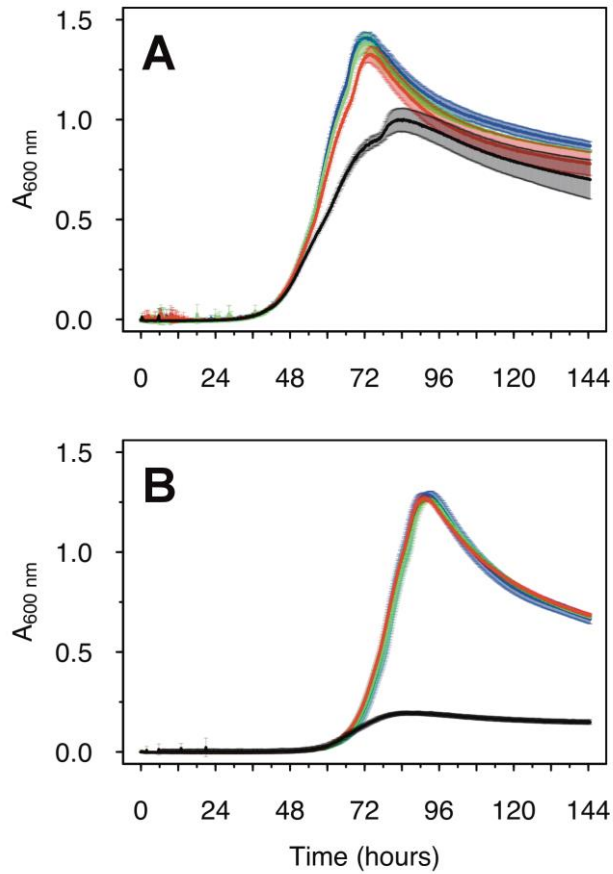
Figure 8. Reductive power (NADH) mitigates the growth inhibitory effects of nitrite in AzwK-3b. Cultures (pre- and main-culture without manganese) were grown in the absence (A) and presence (B) of 5 mM nitrite and supplement of 0, 50, 100 and 200 µM NADH (black, red, green and blue) at the start of the culture.